Electronic Supplementary Material (ESI) for Journal of Materials Chemistry A.

Supplementary Information

Breathable, transparent, waterproof, flexible and high-output triboelectric nanogenerator for sport monitoring and speech recognition

Tong Zheng [1], Guizhong Li[1,*], Linnan Zhang [1], Yong Lei [1]

[1] *College of Mechanical and Electrical Engineering, Wenzhou University, Wenzhou 325035, China.*

Corresponding email: G. Z. Li (liguizhong@wzu.edu.cn).

This file includes:

- Figs. S1 to S33
- Notes S1 to S4
- Tables. S1 to S2.

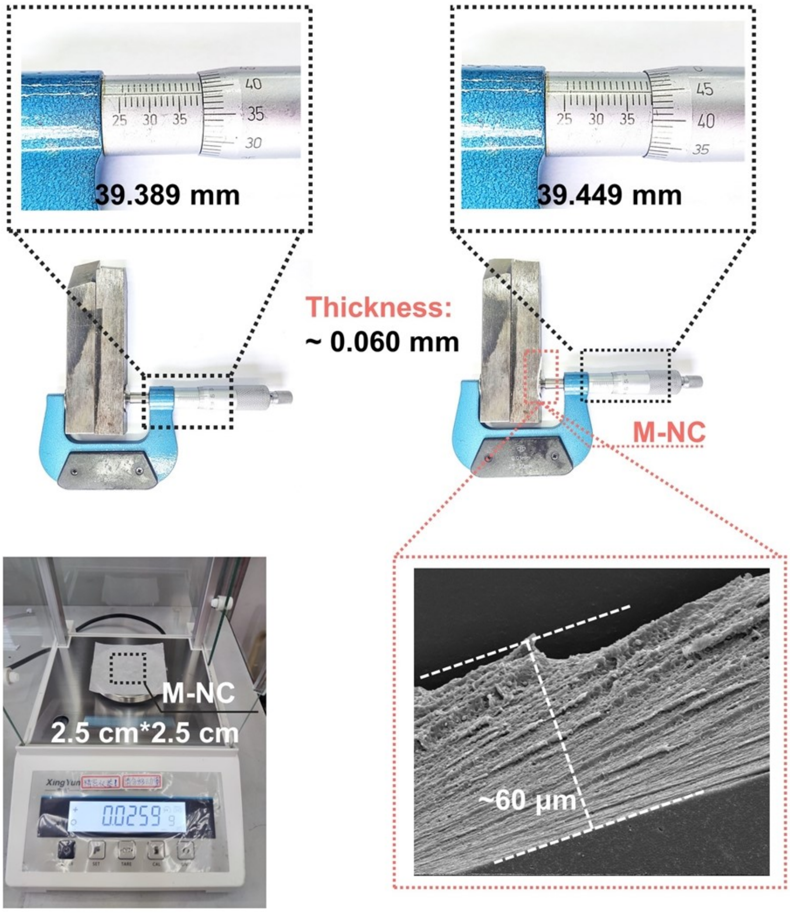

Fig. S1. The thickness and weight of NC/Si RS.

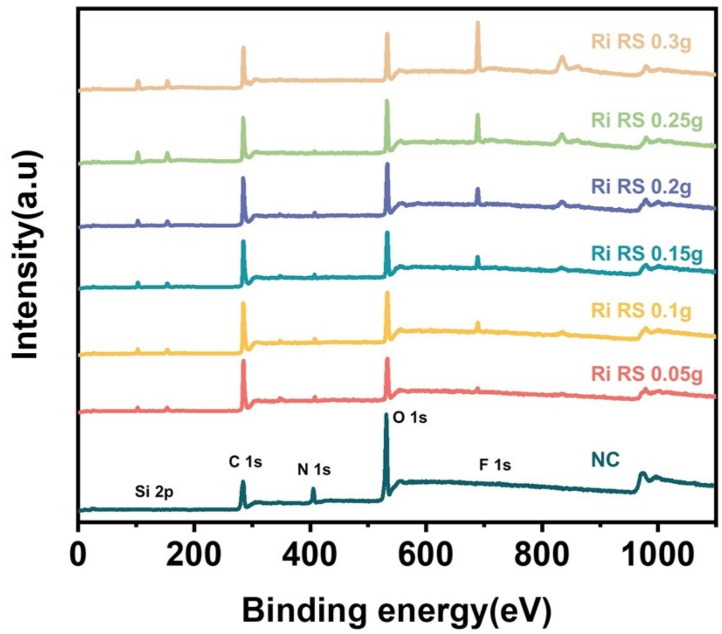

Fig. S2. The XPS results of NC/Si RS with different content Si RS.

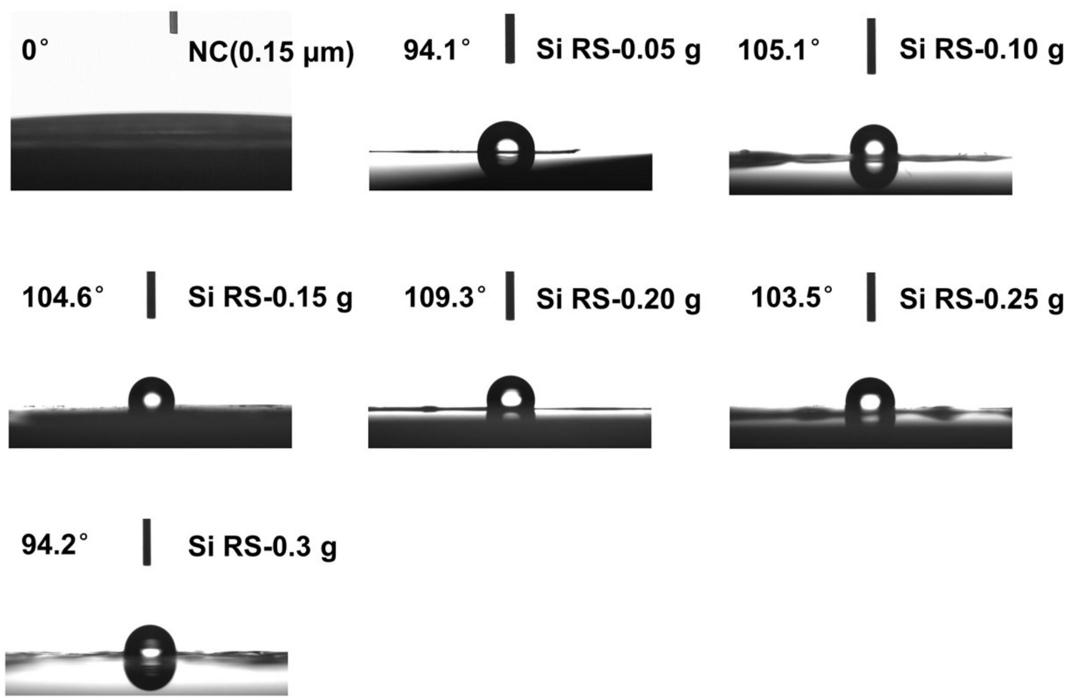

Fig. S3. Difference of water contact angle between NC and NC/Si RSs.

Fig. S4. SEM images of NC/Si RS doped with different Si RS.

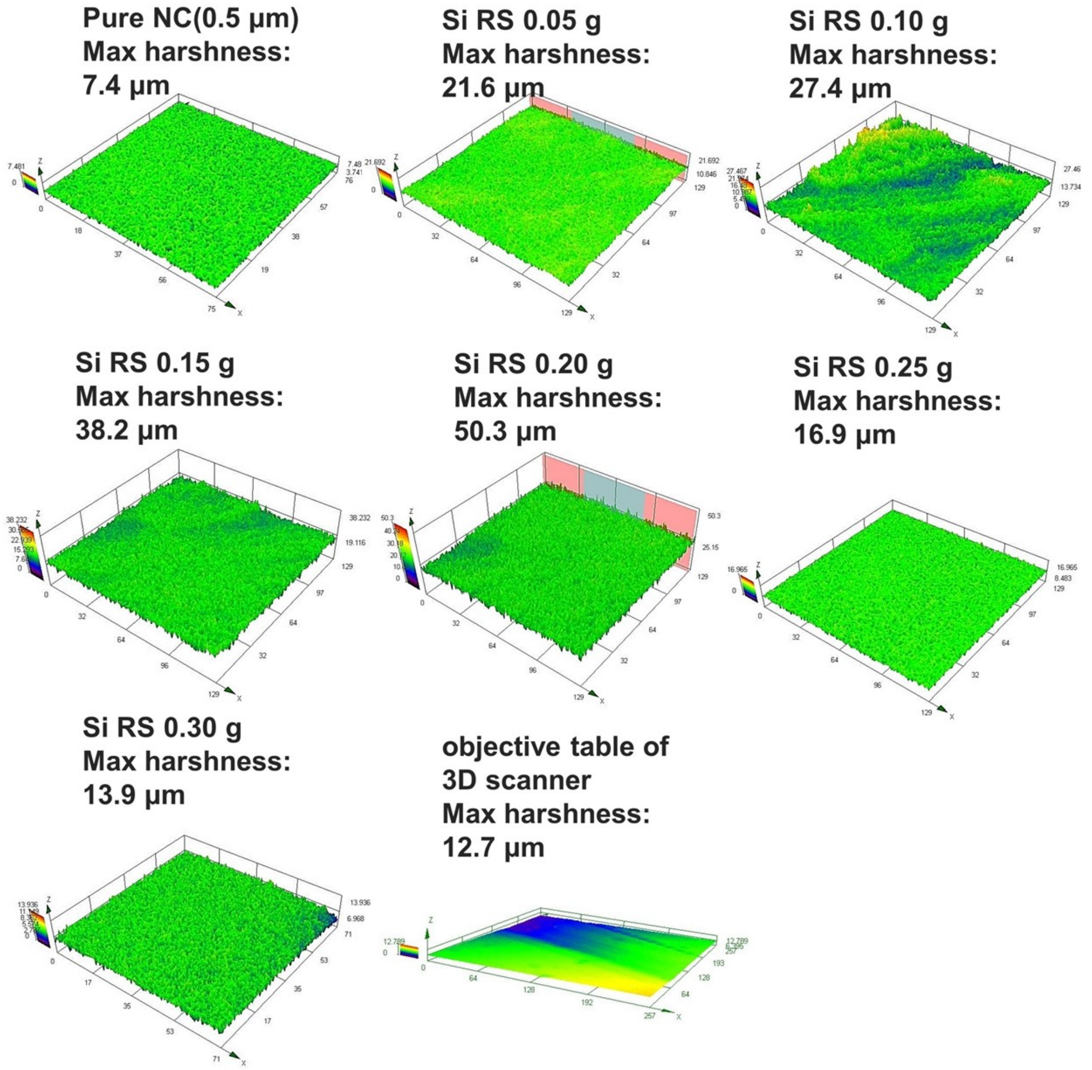

Fig. S5. 3D laser confocal measuring microscope images with different doped Si RS.

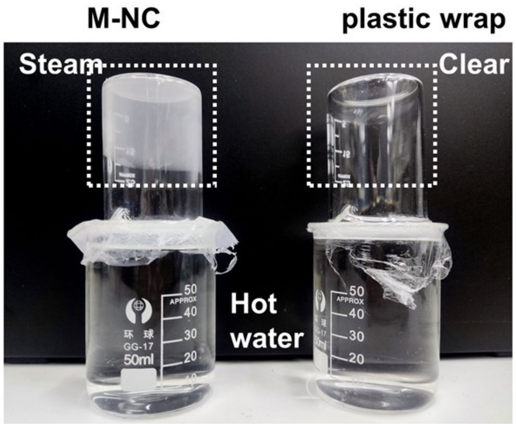

Fig. S6. The difference of NC/Si RS and plastic wrap.

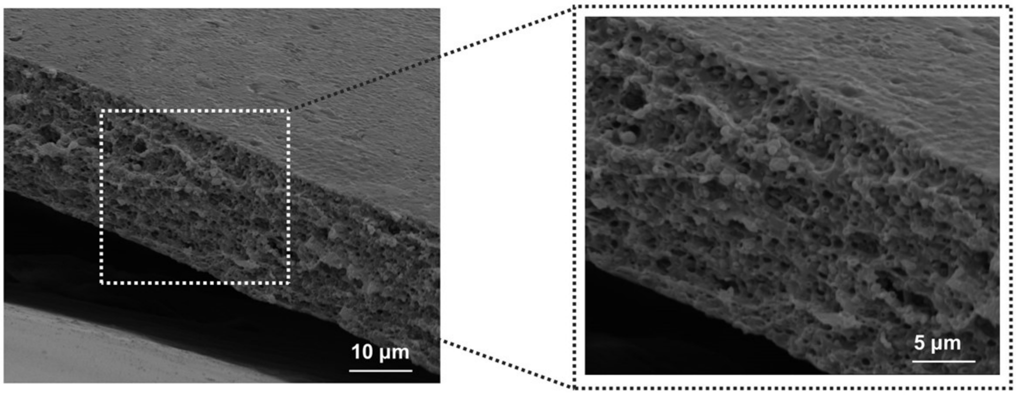

Fig. S7. Porous structure of inner NC/Si RS.

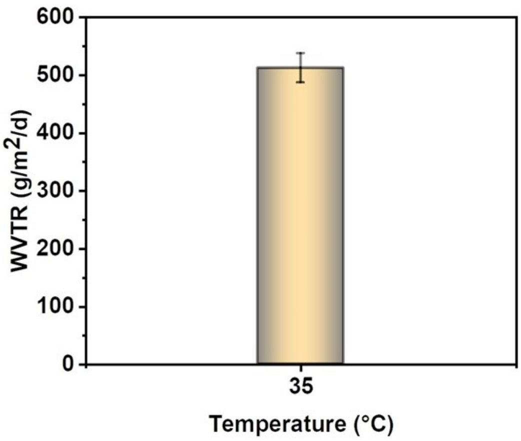

Fig. S8. The WVTR of SNC-TES.

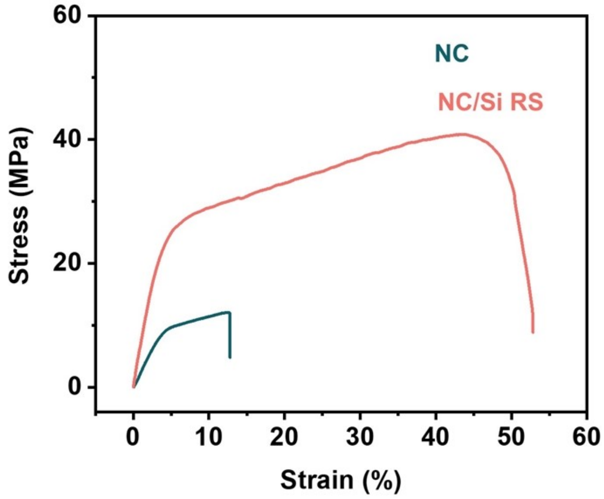

Fig. S9. Typical stress–strain curves of NC/Si RS and NC.

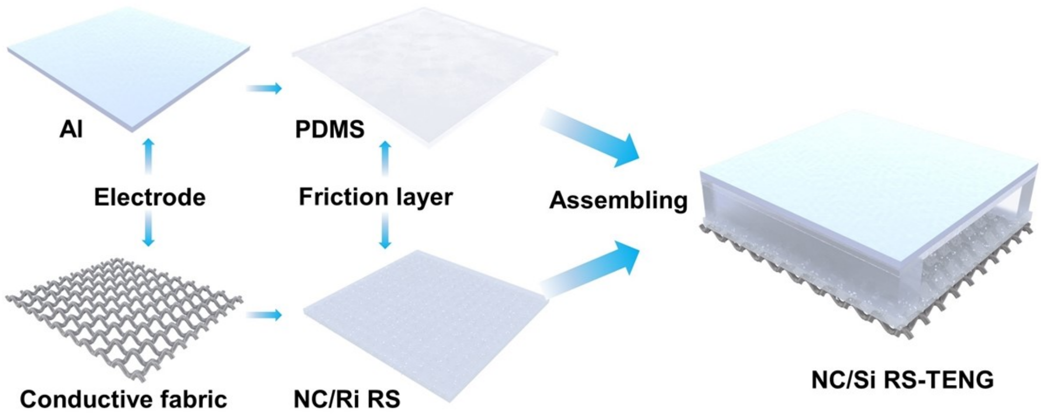

Fig. S10. The preparation process of NC/Si RS-TENG.

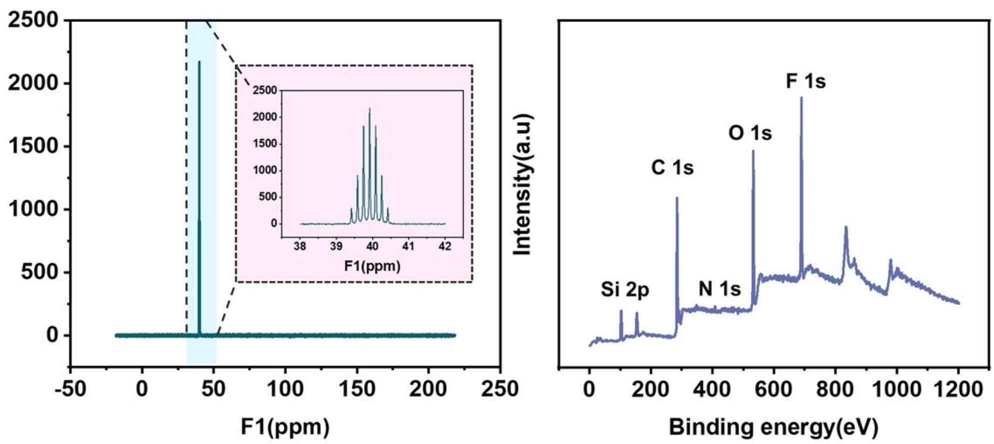

Fig. S11. The 19F NRM and XPS result of the NC/Si RS with 0.3 g Si RS.

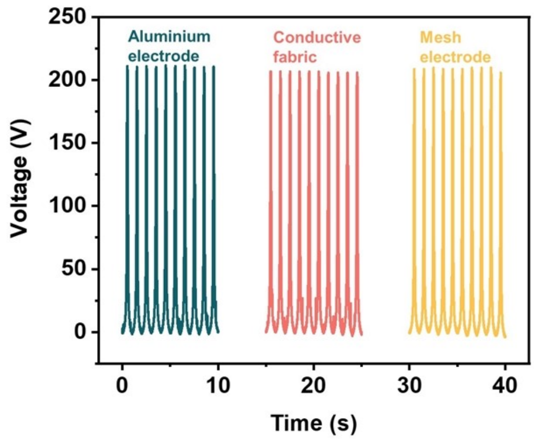

Fig. S12. The output performance of TENG with different material of electrode.

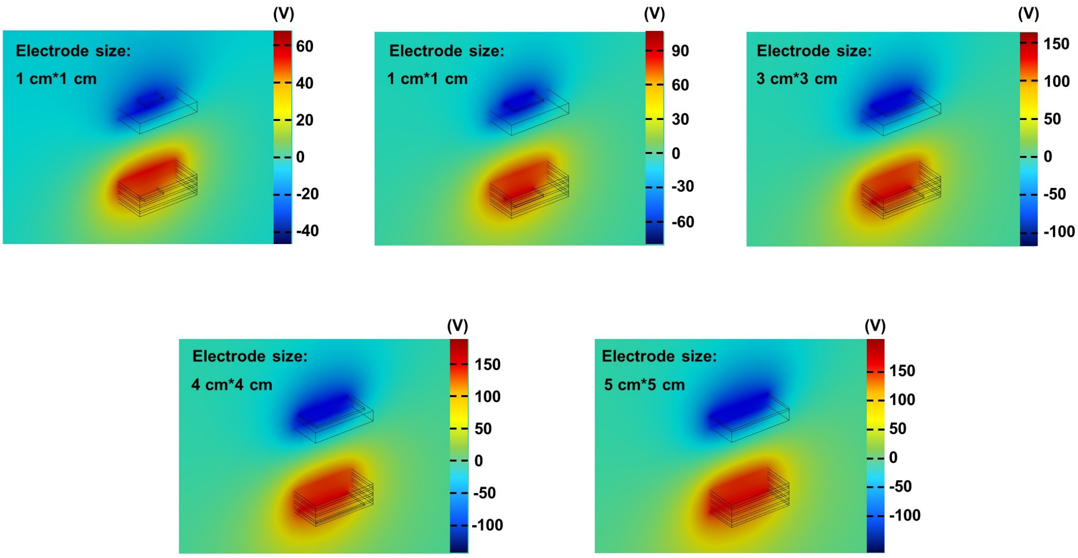

Fig. S13. Finite simulation results of NC/Si RS-TENG equipped with unique area electrodes.

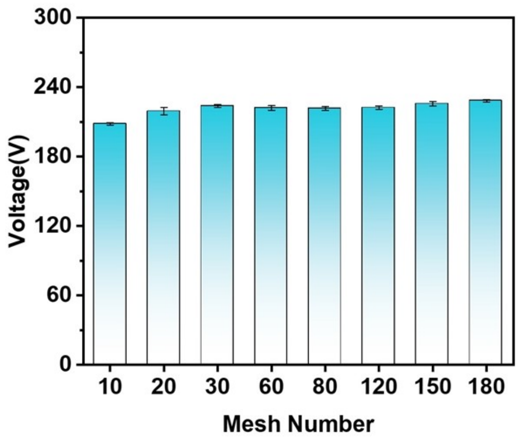

Fig. S14. The output performance of TENG equipped with different mesh number electrode.

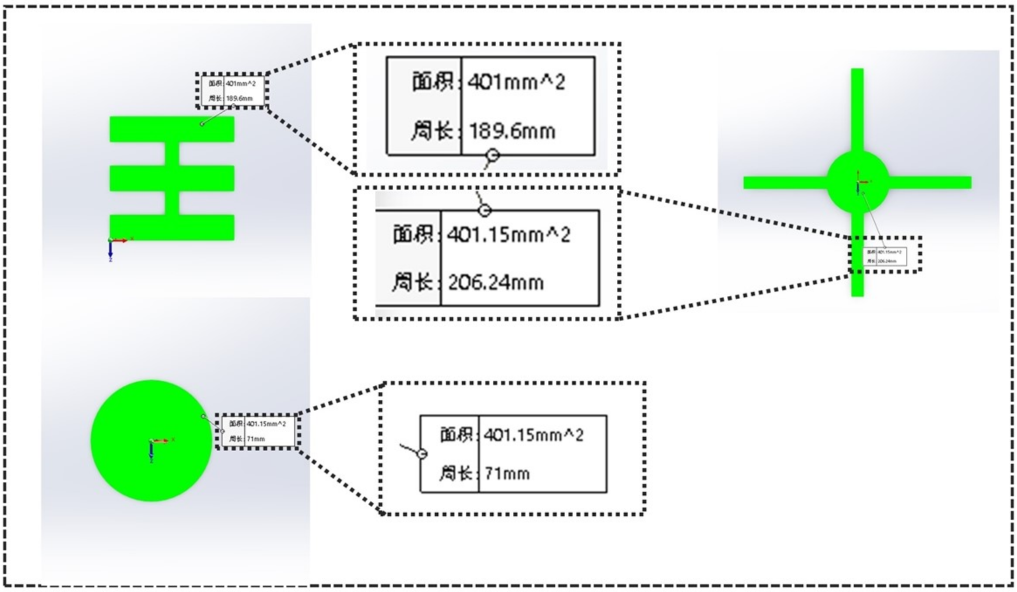

Fig. S15. Designed electrodes, including "king" and "cross" shape electrodes.

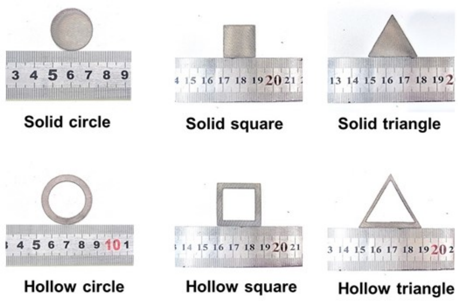

Fig. S16. Electrodes with the same area ($4cm^2$).

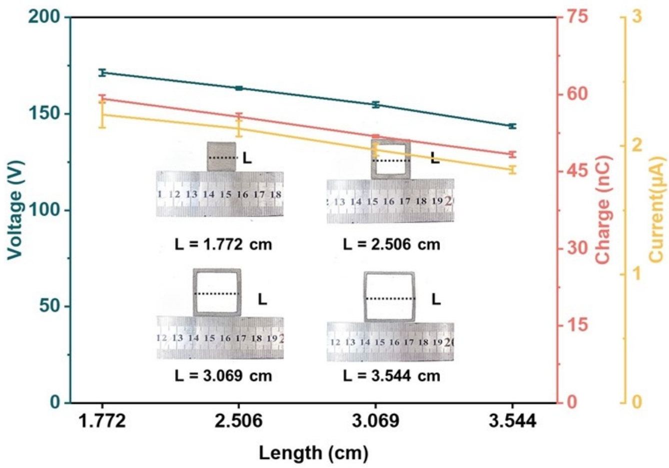

Fig. S17. The output performance of NC/Si RS-TENG equipped with different square electrodes ($4cm^2$).

Fig. S18. The output performance of NC/Si RS-TENG equipped with different circle electrodes ($1cm^2$).

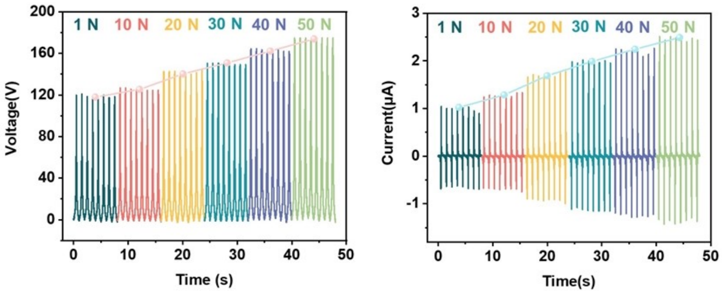

Fig. S19. Output performance of shape adjustable electrode NC/Si RS-TENG (2cm×0.5cm) with different external force.

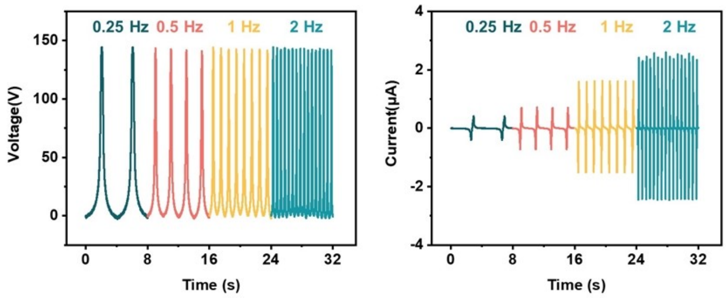

Fig. S20. Output performance of shape adjustable electrode NC/Si RS-TENG (2cm×0.5cm) with different frequencies.

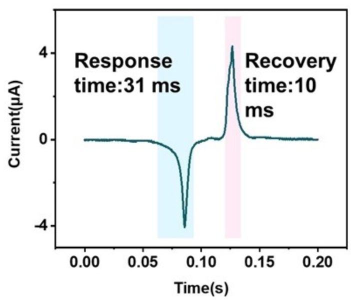

Fig. S21. The response properties of shape adjustable electrode NC/Si RS-TENG.

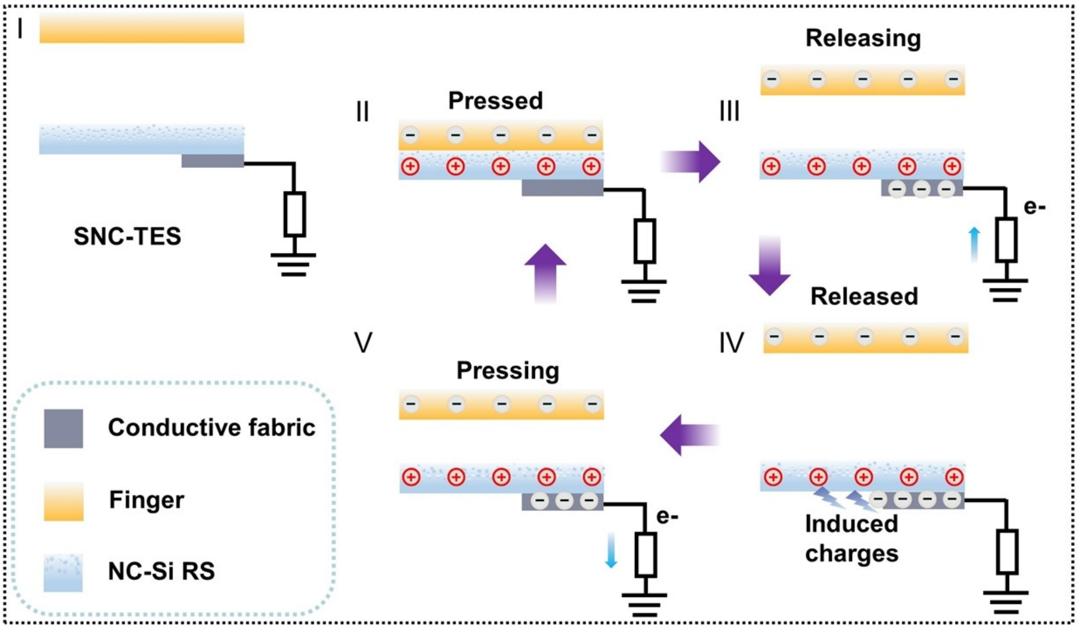

Fig. S22. The working mechanism of shape adjustable electrode SNC-TES.

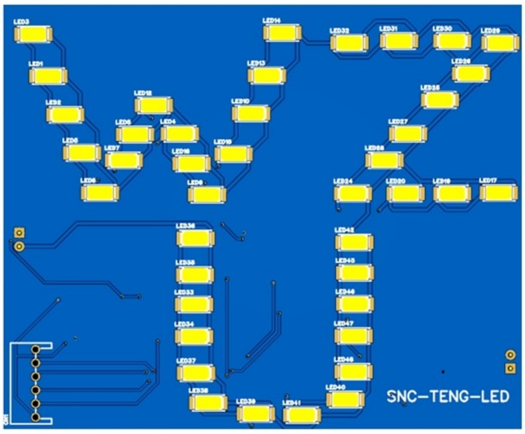

Fig. S23. The PCB broad of LED lights.

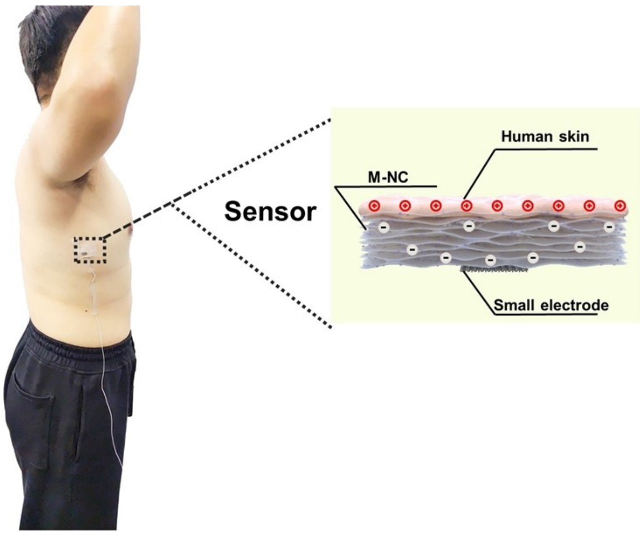

Fig. S24. The pasted position of SNC-TES in human body.

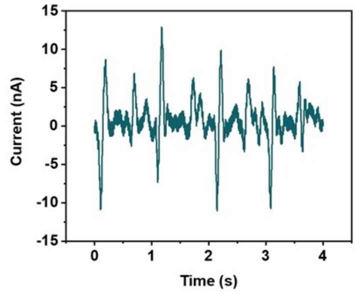

Fig. S25. The signal generated by human swing arm simply.

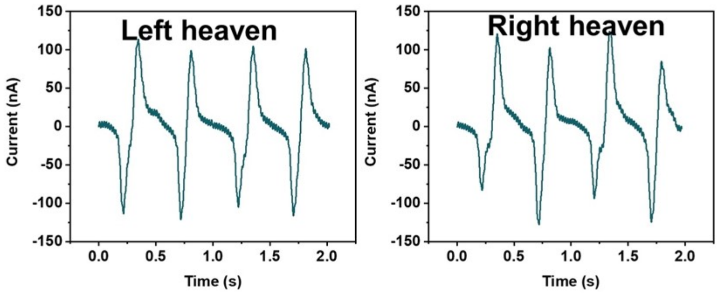

Fig. S26. The signals generated by human' left feet that contacts with ground with unique forces.

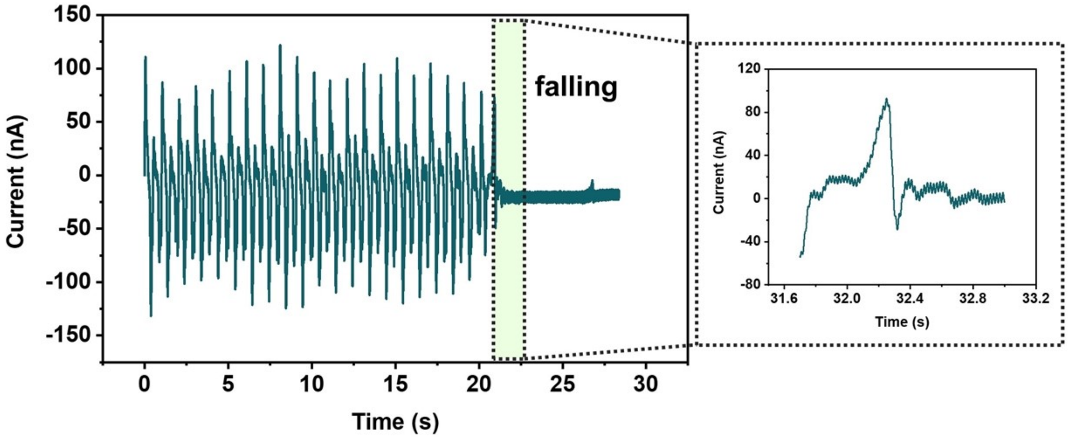

Fig. S27. Imitating the dropping process of human after normal walk about 20 seconds.

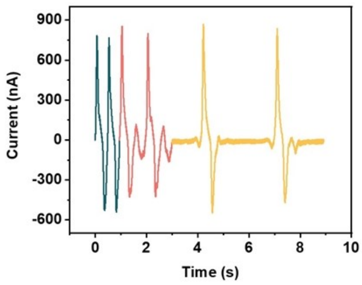

Fig. S28. Signal of human jump with different frequency.

Fig. S29. Frequency spectrums of different motion state (including walk, jog, jump, jump with different heights, jump with different frequencies and wave arm simply).

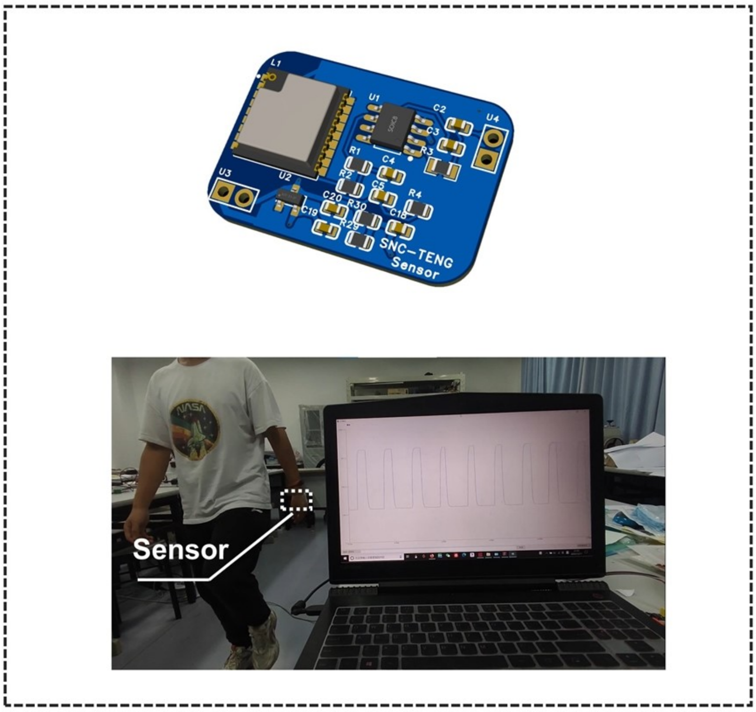

Fig. S30. Demonstration of the potential application of wireless SNC-TES in motion monitor. a) The PCB broads of device. b) The signal generated by human walk.

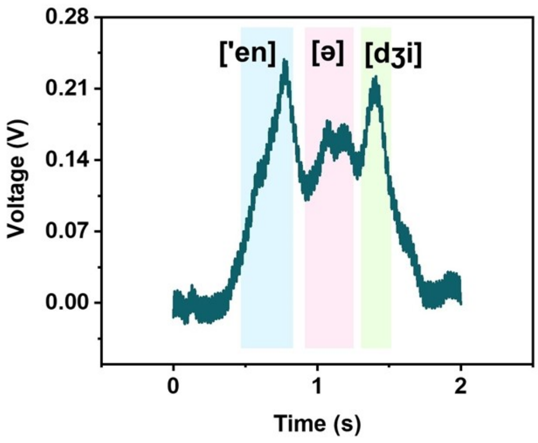

Fig. 31. Syllables and the corresponded signal of the word 'energy'.

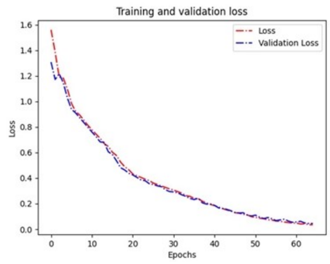

Fig. S32. The loss of training and validation process.

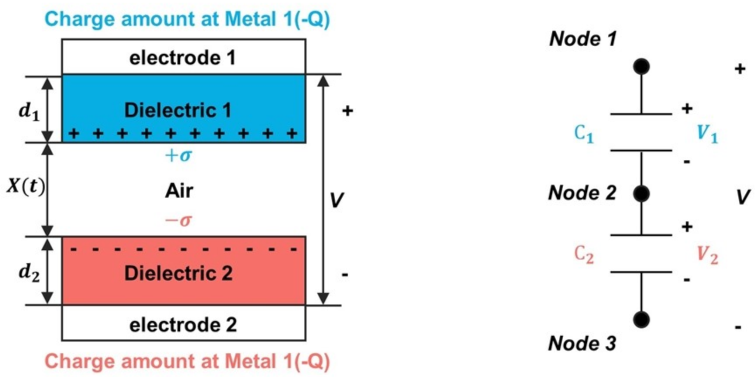

Fig. S33. Theoretical model for dielectric-to-dielectric of TENG.

Note S1: Discussion of the breathability of NC/Si RS

Fig. S6, where two small beakers filled with bowl water at the same volume, the NC/Si RS and plastic wrap were covered to the top surface of small beakers, respectively. At the same time, two large beakers were inverted to small beakers' tops entirely, due to the evaporation of water molecules, steam was continuously released by hot water, those steam can pass through those membranes and attach to the dry and cold beaker wall if those membranes were breathable. The results indicated that the steam can pass through the NC/Si RS, thus the sense of obscure came into being at the surface of the left-top beaker, while the beaker of the right-top still was clear caused by no steam passed. From Fig. S5 can see plainly, steam all adhered to the surface of the plastic wrap.

The WVTR is defined as:

$$WVTR = \frac{(M_2 - M_1)}{S} \quad (1)$$

Where M_1 and M_2 is the weight of the bottle with deionized water before and after testing, respectively, S is the surface area of the membrane.

Note S2: Calculation the instantaneous power density of NC/Si RS-TENG.

The instantaneous power density is calculated based on the equation of:

$$P_D = \frac{UI}{S} \quad (2)$$

Where P_D is the instantaneous power density of NC/Si RS-TENG, U and I is the instantaneous voltage and current, respectively. And S is the contracted area.

Note S3: Discussion the relation between loading frequency and output performance of TENG

Fig. S33 is the theoretical model for dielectric-to-dielectric, the relation between loading frequency and output performance can be derived based on electrodynamics.[1] Thus, the basic equation can be expressed as:

$$V = -\frac{Q}{S\varepsilon_0}\left(d_0 + x(t)\right) + \frac{\sigma x(t)}{\varepsilon_0} \quad (3)$$

While the circuit is in open-circuit condition, charges will not be transferred, thus equation (3) can be expressed as:

$$V_{oc} = \frac{\sigma x(t)}{\varepsilon_0} \quad (4)$$

In short-circuit situation, voltage is zero, and transferred charges are:

$$Q_{sc} = \frac{S\sigma x(t)}{d_0 + x(t)} \quad (5)$$

$$I_{sc} = \frac{dQ_{sc})}{dt} = \frac{S\sigma d_0}{(d_0 + x(t))^2}\frac{dx}{dt} = \frac{S\sigma d_0 v(t)}{(d_0 + x(t))^2} \quad (6)$$

S is the surface area of contact, ε_0 is the dielectric constant of vacuum, σ is the surface charge density, $x(t)$ is the relation of two frictions layer contact and separation, $v(t)$ is the relative speed of two frictions layer. The V_{oc} and Q_{sc} are not influenced by speed, equations (5) and (6) illustrate it clearly. From equation (6), it can be found that the I_{sc} has a close relation with speed. Therefore, the I_{sc} shows the increasing trend with the contact frequency raising.

Note S4: Discussion the working mechanism of SNC-TES.

As illustrates in Fig. S22, the system is in electrostatic equilibrium at the beginning. When the two triboelectric layer contacts, charges are generated due to the contact electrification. Charges are flowed from the ground to the conductive fabric according to the coupling effect of friction electrification and electrostatic induction when the two materials begin to release. It should note that charges can be induced around the electrode area due to electrostatic induction. As a result, an instantaneous current is generated and the electric potential is formed between two materials. The electric potential reaches the maximum when the two materials are released completely. When the two materials are approaching under the effect of external force, charges are transferred from conductive fabric to ground, which leads to a contrary instantaneous current. Contact and separation cyclically can generate periodical triboelectric signal.

Table. S1:

Layer (type)	**Output Shape**	**number of Param**
input_1 (InputLayer)	(None, 5000, 1)	0
conv1d (Conv1D)	(None, 5000, 8)	32
max_pooling1d (MaxPooling1D)	(None, 2500, 8)	0
conv1d_1 (Conv1D)	(None, 2500, 16)	400
max_pooling1d_1 (MaxPooling1	(None, 1250, 16)	0
flatten (Flatten)	(None, 20000)	0
dropout (Dropout)	(None, 20000)	0
dense (Dense)	(None, 32)	640032
dense_1 (Dense)	(None, 6)	198

Total params: 640,662
Trainable params: 640,662
Non-trainable params: 0

Table S2: The comparison of mechanical properties and output performance between NC-TENG and the other works.

Materials	Tensile strength	Elongation at break	Open-circuit voltage	Reference
PLGA/Ag NWs/PVA	3 kPa	~265 %	95 V	[6]
PDMS/Ag-Ni particles	9 Mpa	~92 %	2.12 V	[18]
T-PPM	3 Mpa	~25 %	40 V	[23]
PDMS/H-SiO2(3%)	1.5 Mpa	~200 %	130 V	[43]
CWPT	22 Mpa	~250 %	125 V	[49]
Silicone rubber/Graphenes	80 kPa	~800 %	/	[51]
NC/Si RS	40 Mpa	~45 %	225 V	This work

References

1 S.M. Niu, S.H. Wang, L. Lin, Y. Liu, Y.S. Zhou, Y.F. Hu and Z.L. Wang, *Energy Environ. Sci.*, 2013, **6**, 3576-3583.